Nature of Prominences and their role in Space Weather
Proceedings IAU Symposium No. 300, 2013
B. Schmieder, J.-M. Malherbe & S. T. Wu, eds.

doi:10.1017/S174392131301079X

Rayleigh–Taylor instability in partially ionized prominence plasma

E. Khomenko[1,2], A. Díaz[1,2], A. de Vicente[1,2], M. Collados[1,2] and M. Luna[1,2]

[1]Instituto de Astrofísica de Canarias, 38205 La Laguna, Tenerife, Spain
email: khomenko@iac.es

[2]Departamento de Astrofísica, Universidad de La Laguna, 38205, La Laguna, Tenerife, Spain

Abstract. We study Rayleigh–Taylor instability (RTI) at the coronal–prominence boundary by means of 2.5D numerical simulations in a single-fluid MHD approach including a generalized Ohm's law. The initial configuration includes a homogeneous magnetic field forming an angle with the direction in which the plasma is perturbed. For each field inclination we compare two simulations, one for the pure MHD case, and one including the ambipolar diffusion in the Ohm's law, otherwise identical. We find that the configuration containing neutral atoms is always unstable. The growth rate of the small-scale modes in the non-linear regime is larger than in the purely MHD case.

Keywords. Instabilities; Numerical simulations; Chromosphere; Magnetic fields; Prominences.

Solar prominences are blocks of cool and dense chromospheric-type plasma remaining stable for days, or even weeks, in the solar corona. Despite the global stability, prominences are extremely dynamic at small scales, showing a variety of shapes, moving with vertical and horizontal threads. Berger *et al.* (2010) find large-scale 20–50 Mm arches, expanding from underlying corona into the prominences. At the top of these arches, at the border between the corona and the prominence, there are observed dark turbulent upflowing channels of 4-6 Mm maximum width with a profile typical for the Rayleigh–Taylor (RT) and Kelvin–Helmholtz (KH) instabilities (Berger *et al.* 2010; Ryutova *et al.* 2010). The upflows rise up to 15–50 Mm, with an average speed of 13–17 km s^{-1}, decreasing at the end. Lifetimes of the plumes are about 300–1000 sec. From the theoretical point of view, the existence of the instabilities at the interface between the prominence and the corona is easily explained since the two media have clearly different densities, temperatures and relative velocities. Recent numerical simulations of the RTI by Hillier *et al.* (2012), including a rising buoyant tube in a Kippenhahn–Schlüter prominence model show a good agreement with observations. Nevertheless, prominence plasma is expected to be only partially ionized. The presence of a large number of neutrals must affect the overall dynamics of the plasma. Linear theory of RTI and KHI in the partially ionized plasma has been recently developed by Soler *et al.* (2012); Díaz *et al.* (2013) showing that there is no critical wavelength as in the purely MHD case ($\lambda_c = B_0^2 \cos^2\theta/(\rho_2 - \rho_1)/g$; B_0 and θ are magnetic field strength and inclination, $\rho_2 - \rho_1$ is density contrast between the two media, g is gravity), and perturbations in all the wavelength range are always unstable. The aim of our work is to model the dynamics of RTI in the partially ionized prominence plasma in the non-linear regime.

We simulate a small portion of the interface between prominence and corona, of the size of 1×1 Mm. The initial stratification of the pressure and density is in hydrostatic equilibrium for a given temperature. The equilibrium magnetic field, $\vec{B}_0$, is homogeneous and does not influence the force balance. The plasma is perturbed in the XZ plane, the

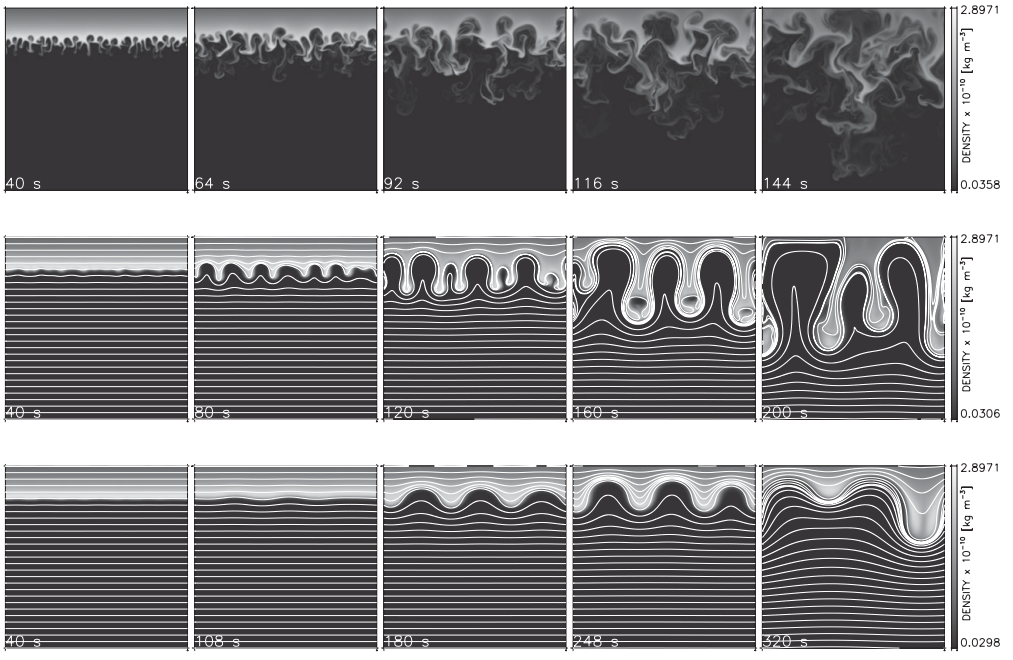

Figure 1. Top: Time evolution of density in the "ambipolar" simulation with $\theta = 90°$. Middle: same for the simulation with $\theta = 89°$. White lines are projections of magnetic field lines into XZ perturbation plane. Bottom: same for the simulation with $\theta = 88°$.

magnetic field vector is initially in XY plane, making an angle with X axis. We consider 3 simulation runs with $\vec{B}_0$ at $\theta = 90°$ to X axis (i.e. normal to the XZ plane), $\theta = 89°$ and $88°$. The following parameters of the equilibrium configuration were taken: $T_{\rm cor} = 400$ kK, $T_{\rm prom} = 5$ kK; $\rho_{\rm cor} = 3.7 \times 10^{-12}$ kg m^{-3}, $\rho_{\rm prom} = 2.9 \times 10^{-10}$ kg m^{-3}, and $B_0 = 10$ G. This provides prominence neutral fraction (the ratio of neutral density to the total density, ρ_n/ρ) of 0.9 and the ambipolar diffusion coefficient of $\eta_A = 2.3 \times 10^8$ m^2 s^{-1}. To initiate the instability we perturbed the position of the interface by a multi-mode perturbation containing 25 modes with wavelengths in the range $\lambda = 10 \div 250$ km. The resolution of the simulations was 1 km in each spatial direction. Such high resolution is expected to be necessary to study non-ideal plasma effects.

After subtracting the equilibrium conditions, we solve numerically the quasi-MHD equations of conservation of mass, momentum, internal energy, and the induction equation by means of our code MANCHA (Felipe *et al.* 2010; Khomenko & Collados 2012) with the inclusion of the physical ambipolar diffusion term in the equation of energy conservation and in the induction equation. We evolve the ionization fraction in time by Saha equation, as a first approximation. Our code uses hyperdiffusivity for stabilizing the numerical solution. To assure that the numerical diffusivity (whose action resembles the physical diffusivity) does not affect the results of the simulations, we kept the amplitude of artificial hyperdiffusive terms 2-3 orders of magnitude lower than the physical ambipolar diffusion so that the characteristic time scales of action of the former are orders of magnitude large. For each field inclination we perform two identical simulations, one for the purely MHD case and one with the ambipolar term switched on.

Figure 1 gives the time evolution of density perturbation in the "ambipolar" simulations for the three field inclinations. The case of the magnetic field normal to the plane of the instability ($\theta = 90°$) is analogous to a purely hydrodynamical case since there

https://doi.org/10.1017/S174392131301079X Published online by Cambridge University Press

is not cut-off wavelength. Indeed, the simulation shows the development of very small scales. The comparison of the "MHD" and "ambipolar" simulations (not shown in the Figure) reveals different (but statistically equivalent, as is shown below) particular form of the turbulent flows, since the ambipolar diffusion, acting on small scales, forces their different evolution. The density variations have a pronounced asymmetry between the large-scale upward rising bubbles and small-scale downflowing fingers, caused by the mass conservation. Such asymmetric behavior can possibly explain the preferred detection of the larger-scale upward rising bubbles in observations (Berger *et al.* 2010).

By just rotating the field by 1° in XY plane the scales developed in the simulation are significantly changed (middle panels of Fig. 1, $\theta = 89°$), small scales disappear and only few big drops are developed after about 200 sec of the simulation. The small scales can not develop the instability because of the cut-off induced by the magnetic field, $\lambda_c \approx 38$ km, for our equilibrium configuration and $\theta = 89°$. While not completely damped as in the purely MHD case, the growth rate of small scales is still very low compared to large scales, see the results by Díaz *et al.* (2013). One can appreciate from the figure that at $t = 40$ sec the dominant wavelength is around $\lambda \approx L/9$ km, while at $t = 120$ sec it becomes $\lambda \approx L/6$ and finally after $t = 200$ sec the dominant wavelength is equal to $\lambda \approx L/3$, being $L = 1$ Mm the size of the simulation box. During the evolution of the instability, the horizontal magnetic field component increases below and above the drops as the field gets compressed by the flows. The increase of the field produces a local increase of the cut-off wavelength, contributing additionally to the damping of small scales. Moreover, small scales tend to disappear with time due to non-linear interaction of harmonics with larger scales, as was already demonstrated by other numerical works on the RTI (Jun *et al.* 1995). Similar trend is observed in the simulation with $\theta = 88°$, in the bottom panels of Fig. 1. In this case, the critical wavelength is $\lambda_c \approx 155$ km, and, accordingly, the developed scales are even larger. Note that, at lower field inclinations, the evolution takes progressively more time, since the tension force by the magnetic field slows down the development of the instability, in agreement with the linear theory.

The velocity of flows lie in the range of 10–20 km s^{-1}, similar to observations. The downflows are observed in about 2/3 of all points, and upflows occupy the remaining 1/3 but the upflow velocities are, on average, larger. The comparison of the flows in the "ambipolar" and the "MHD" simulations in approximately linear stage of the RTI (first few tens of sec of the simulation), reveals slightly larger velocities in the "ambipolar" simulations, i.e. this case is slightly more unstable.

To analyze the stability of different scales in the non-linear regime of the RTI, at each time moment t we calculated the power as a function of the horizontal wave number k_x by fourier-transforming in space a portion of the snapshot of pressure variations around the discontinuity, and by averaging the power for the vertical k_z wave number to decrease the noise. We then divided the "ambipolar" power map by the corresponding "MHD" map for each pair of the simulations, $\theta = 90°$, 89° and 88°. The result is given at the left panels of Fig. 2, while the right panel shows the time-averages of the relative power maps. In the case of the field directed normal to the perturbation plane ($\theta = 90°$), we do not observe any significant change in power between the "ambipolar" and "MHD" cases. The relative power fluctuates in time, but the average remains around one for all harmonics (upper left panel). This behavior is already anticipated from the linear analysis (Díaz *et al.* 2013). The relative power is significantly different to that in the cases with $\theta = 89°$ and 88°. Now there is a clear increase in the growth rate of the small-scale harmonics in the "ambipolar" simulations compared to the "MHD" ones. The growth rate of the large-scale harmonics is the same in both cases. The change in the behavior happens at about $\lambda \sim 30$ km for the $\theta = 89°$ case, and at $\lambda \sim 100$ km for the $\theta = 88°$ case, both

https://doi.org/10.1017/S174392131301079X Published online by Cambridge University Press

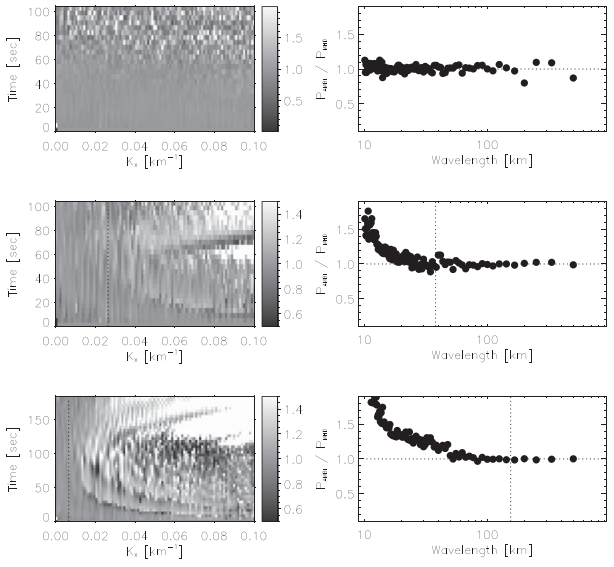

Figure 2. Fourier analysis of scales developed in the simulations. Left: relative power of the "ambipolar" vs "MHD" simulation as a function of horizontal wave number along the discontinuity, k_x, and time. Whiter colors mean that the "ambipolar" simulation has more power. Right: time average of the relative power from the panels on the left. Top: $\theta = 90°$. Middle: $\theta = 89°$. Bottom: $\theta = 88°$. In the last two cases, the vertical dotted lines at the right panels mark the cut-off wavelength $\lambda_c = 38$ and 155 km, correspondingly.

numbers being close to the corresponding cut-off wavelengths λ_c. This result confirms and extends the conclusion from the linear theory that all RTI modes become unstable when the presence of neutral atoms is accounted for in the analysis. We obtain up to 50% increase of the small-scale harmonics growth rate for the $\theta = 89°$ case and up to 90% increase for the $\theta = 88°$ case. Our simulations show that partial ionization of prominence plasma measurably influences its dynamics and must be taken into account in future models.

Acknowledgements

This work contributes to the deliverables identified in FP7 European Research Council grant agreement 277829, "Magnetic connectivity through the Solar Partially Ionized Atmosphere", whose PI is E. Khomenko.

References

Berger, T. E., Slater, G., Hurlburt, N., *et al.* 2010, *ApJ*, 716, 1288
Díaz, A. J., Khomenko, E., & Collados, M. 2013, *A&A*
Felipe, T., Khomenko, E., & Collados, M. 2010, *ApJ*, 719, 357
Hillier, A., Berger, T., Isobe, H., & Shibata, K. 2012, *ApJ*, 746, 120
Jun, B.-I., Norman, M. L., Stone, & J. M. 1995, *ApJ*, 453, 332
Khomenko, E. & Collados, M. 2012, *ApJ*, 747, 87
Ryutova, M., Berger, T., Frank, Z., Tarbell, T., & Title, A. 2010, *Solar Phys.*, 267, 75
Soler, R., Díaz, A. J., Ballester, J. L., & Goossens, M. 2012, *ApJ*, 749, 163

https://doi.org/10.1017/S174392131301079X Published online by Cambridge University Press